energies

MDPI

Article

STGCN- and IMOPSO-PSD-Based Optimization of Unit Operation Modes of Asynchronous Networking Sending-End Power Systems with High-Penetration Renewable Energy

Dan Zhang [1], Yan Liu [2,*], Xuhui Zhu [2], Weixin Wang [2], Kaiyuan Yu [1] and Keyi Xu [2]

[1] Yunnan Electric Power Dispatching and Control Center, China Southern Power Grid Yunnan Power Grid Co., Ltd., Kunming 650032, China
[2] Department of Electrical Engineering, North China Electric Power University, Baoding 071003, China
* Correspondence: y.liu@ncepu.edu.cn

Abstract

To address the coordinated control need for optimizing clean power transmission and ensuring stable operation of asynchronous sending-end power systems with high-penetration renewable energy, this paper proposes a fast optimization method for unit operation modes based on spatio-temporal graph convolutional network (STGCN) and Improved Multi-Objective Particle Swarm Optimization–Power System Department Software (IMOPSO-PSD) method. First, a Unit Operation Mode Optimization (UOMO) model is established, which aims to maximize the DC transmission capacity and renewable energy accommodation capacity while minimizing the voltage support imbalance degree. Second, an STGCN optimization framework integrated with system operation security constraints and loss feedback of optimization objectives is designed, transforming the solution of UOMO model into the prediction of the optimal unit operation mode. Finally, a fast optimization process for unit operation modes based on STGCN and IMOPSO-PSD is presented, where the simplified IMOPSO-PSD is used to rapidly refine and verify the prediction results of the STGCN. Simulation results based on the modified IEEE 39-bus system show that the proposed method effectively integrates fast spatiotemporal feature extraction and prediction of STGCN with precise constraint verification of IMOPSO-PSD, thus ensuring the rationality and applicability of the optimization results for unit operation modes.

Keywords: asynchronous sending-end power; high-penetration renewable energy; STGCN; IMOPSO; unit operation mode optimization

Check for updates

Academic Editor: Giovanni Lutzemberger

Received: 7 January 2026
Revised: 12 February 2026
Accepted: 21 February 2026
Published: 25 February 2026

Copyright: © 2026 by the authors. Licensee MDPI, Basel, Switzerland. This article is an open access article distributed under the terms and conditions of the Creative Commons Attribution (CC BY) license.

1. Introduction

To address the challenge of long distance between primary energy-rich regions and load centers, China has implemented the strategy of "West-to-East Power Transmission and National Grid Interconnection", forming a power grid structure with large-scale cross-regional AC/DC interconnection. As an important sending-end grid of the southern corridor for "West-to-East Power Transmission", Yunnan Power Grid, which is rich in renewable energy resources, has achieved asynchronous interconnection with the main grid of China Southern Power Grid to meet the demand for large-scale and wide-range accommodation of renewable energy [1]. However, with the continuous increase in the proportion of renewable energy integration, the capacity of synchronous generators connected with Yunnan Power Grid has decreased, the system mechanical inertia has dropped significantly, and both the frequency regulation capability and voltage support capability

have been significantly weakened [2]. Meanwhile, renewable-energy-generating units suffer from weak disturbance rejection, low overload capacity, and insufficient tolerance to frequency and voltage deviations. The superposition of these factors poses a serious threat to the operational security of the sending-end system and also restricts the effective improvement of the DC delivery scale of clean energy. Therefore, there is an urgent need for a safe and efficient operation optimization and adjustment method that can synergistically improve renewable energy accommodation and power transmission amount of the DC transmission lines on the premise of ensuring the operational security of the asynchronous interconnected sending-end system.

Operation optimization and adjustment is a common measure for power grid dispatch departments at all levels to improve the operational security and economic efficiency of the system. Many studies related to improving the operational performance of power grids have employed various optimization techniques to minimize operational costs and losses or to improve the voltage profile and renewable energy accommodation. Focusing on the coordinated operation of the regulated power supply and the renewable energy source, Reference [3] proposes a joint optimization model for multi-energy complementary clean energy bases. Based on the long-term load and power generation data of renewable energy base typical scenarios in western China, it is demonstrated that the model is effective in accommodating green power and the economic viability of investment as well. In [4], a day-ahead optimization model of active distribution network is established to coordinate the operation of distributed renewable energy generation, energy storage device and interruptible load in order to realize the maximum consumption of distributed green power and the economical operation of distribution network and the model is solved by means of adaptive particle swarm optimization (APSO). Combined cooling, heating and power (CCHP) systems, as typical distributed multi-energy supply systems in the energy sector, are widely favored for their high energy utilization efficiency. A dual-focused optimization model is proposed in [5] to address economic efficiency and environmental sustainability concurrently, where an improved particle swarm optimization (IPSO) is employed to solve the model. Taking tap changing voltage regulators and reactive power capability of PVs into account, Reference [6] develops a model based on Whale Optimization Algorithm to minimize voltage deviations and active power losses of a low-voltage distribution system during the heavy load operation scenario. The Osprey Optimization (OO) is applied in [7] to the optimal operation of a modified CIGRE benchmark microgrid in order to minimize generation cost and losses when the load of the microgrid is supplied with conventional energy, renewable energy and energy storage system. Case studies on normal operation and generator outage demonstrate the advantages of OO over the conventional PSO. Considering the uncertain factors in power system operation, such as initial data and dynamic changes in the system, Reference [8] constructs a neural analytical network model to optimize the power system operation mode, so as to reduce active power losses while improving the adaptability of system operation. With an integrated simulated annealing algorithm (SA) and deep reinforcement learning (DRL), Reference [9] proposes a multi-objective optimization model to address distribution network efficiency reduction due to high reactive power losses. The model transforms the optimization of distribution network operation mode into a Markov decision process, which significantly improves decision-making efficiency. In power systems with a high penetration of renewable energy, the optimal allocation of reserve capacity has gradually become a research hotspot to address the adequacy risks caused by the frequent fluctuations in renewable energy output. Incorporating both economic cost and multi-resource physical constraints, Reference [10] provides a hierarchical hybrid reinforcement learning framework to optimize dispatching of multi-type resource reserve in terms of wind power prediction deviations. Reference [11]

proposes a novel method for utility-level battery control in distribution grids, which integrates reinforcement learning (RL) into model predictive control (MPC). The proposed approach considers look-ahead constraints on the battery state of charge while forming a fast and real-time battery control strategy. Simulation results demonstrate that the proposed method outperforms the conventional MPC and other safe RL schemes in terms of both cost performance and constraint violations. Optimization of power grid operation relies on optimal power flow (OPF) calculations with specific objectives. Recently, neural networks (NN) have shown great potential for solving large-scale OPF problems. To enhance the interpretability and reliability of NN-based methods, Reference [12] proposes a transparent neural network solver for the OPF problem. It explicitly explains the input–output relationship by performing Taylor expansion on the Karush–Kuhn–Tucker (KKT) conditions of the OPF model and deriving network weights. Numerical results demonstrate that the proposed solver achieves high efficiency, strong generalization, superior accuracy, and reliability.

Under the new power system paradigm, the large-scale integration of high-penetration renewable energy endows power grids with pronounced spatio-temporal coupling characteristics, which are precisely the advantage of spatio-temporal graph convolutional network (STGCN) modeling. STGCN is a deep-learning model specifically designed to process graph-structured data that evolves over time, which is good at simultaneously capturing the features and dependencies of data in both the spatial (graph structure) and temporal (sequence) dimensions. Currently, applications of STGCN in power systems are mainly concentrated in the fields of renewable energy generation and load forecasting, as well as power system stability analysis and assessment [13–19]. Reference [13] employs STGCN to encode multi-input data and leverages transformers to capture temporal dependencies, achieving high-precision short-term load forecasting for integrated energy systems. In Reference [14], an improved STGCN is adopted to extract deep spatial–temporal features of wind power so as to improve the accuracy of ultra-short-term power forecasting. Reference [15] achieves low root mean square error prediction by combining STGCN with gated linear units to capture spatial and temporal characteristics across multiple photovoltaic power stations. In the field of system stability assessment, Reference [16] demonstrates that STGCN combined with residual networks can be applied to short-term voltage stability evaluation in regional power grids. Reference [17] combines the self-attention mechanism with STGCN, enhancing the model's generalization ability against changes in topological structure, thereby making it suitable for frequency stability prediction. To address the problems of dynamic reconfiguration and voltage regulation in unbalanced three-phase distribution systems, Reference [20] proposes a physics-informed STGCN, which can accurately predict the status of tie switches/sectionalizers and the tap positions of voltage regulators, paving the way for the efficient solution of refined adjustment schemes through planning algorithms in subsequent steps. Simulations demonstrate that the proposed method can effectively reduce distributed energy resource (DER) curtailment and voltage deviation. In comparison, research on the application of STGCN to the optimal operation of power systems remains relatively limited, mainly due to the challenges in comprehensively and accurately modeling the operational security constraints of power systems.

In summary, fruitful research achievements have been made on the optimal operation of power systems or multi-energy systems. However, existing studies pay relatively little attention to the optimal operation of asynchronously interconnected systems, especially on how to coordinate the operational security of the sending-end system itself and the power delivery demand of the outgoing DC links. Therefore, the research challenge addressed in this paper is as follows: for the DC sending-end systems with asynchronous interconnection, to develop a fast optimization method for system operation that satisfies

the required security margins of voltage and frequency and can maximize the delivery of clean energy through DC lines. The objective is to meet the demand for secure and flexible adjustment of unit operation modes caused by load and the frequent fluctuations in renewable energy generation. Against the above background, this paper proposes a fast optimization method for unit operation mode of asynchronous networking sending-end power systems with high-penetration renewable energy based on STGCN and IMOPSO-PSD. Its main innovations are as follows: by embedding operational security constraints and multi-objective guidance terms of unit operation modes into STGCN, a prediction model for unit operation mode of the sending-end system is established. Then, through the refining and verification employing the simplified IMOPSO-PSD process, the optimal unit operation mode of the sending-end system is obtained.

The remainder of this paper is organized as follows. First, Section 2 describes the formulation of UOMO model based on the support capability adjustment of the sending-end system in asynchronous interconnected grids. Second, Section 3 establishes a fast optimization framework for unit operation mode of the sending-end power system based on STGCN, in which solving UOMO is transformed into a prediction problem of the optimal operation mode. Furthermore, Section 4 elaborates the workflow of fast unit operation mode optimization integrating STGCN and IMOPSO-PSD. Subsequently, Section 5 demonstrates the model application on the modified IEEE 39-bus system. Finally, the conclusions of this paper and discussions on future work are presented.

2. Unit Operation Mode Optimization (UOMO) Model Based on Support Capability Adjustment of the Sending-End System

From the perspective of preventive control, improving the voltage and frequency support capability of the sending-end system plays a fundamental role in ensuring the operational security of asynchronous interconnection channels and enhancing the delivery level of clean energy. On the one hand, uneven distribution of voltage support capability may lead to the risk of systemic cascading failures triggered by unit disconnection in regions with weak support capability. On the other hand, when evaluating the frequency support capability of sending-end power systems in asynchronous interconnected grids, in addition to common disturbance scenarios such as fluctuations in load and renewable energy generation, special attention should be paid to the impacts imposed on the system by severe faults such as large-capacity DC blocking. Therefore, this paper adopts the multiple renewable energy stations short circuit ratio (MRSCR) as an index to quantify the voltage support capability of the sending-end system [21]. Meanwhile, the maximum transient frequency deviation under active power deficit and surplus accidents is adopted to characterize the frequency support capability [22]. On this basis, UOMO model based on the support capability adjustment of the sending-end system is established. Its core idea is, by optimally adjusting the output of synchronous generators and renewable energy units in the sending-end system, the power via DC external transmission and the accommodation capacity of renewable energy are maximized, while the imbalance degree of voltage support capability is minimized. The objective function and constraints of the model are elaborated in detail as follows.

2.1. Objective Function

Focusing on the system operation state at a given moment, the objective function of UOMO model based on the support capability adjustment of the sending-end system is

given by Equation (1). Decision variables are the outputs of synchronous generators and renewable energy units in the sending-end system.

$$\max(F_1, F_2, -VSID) \tag{1}$$

2.1.1. DC External Transmission Power F_1

The DC external transmission power level F_1 consists of the active power flow level F_{DC} of the DC transmission channels in the asynchronously interconnected system and the heavy-load severity F_P of the sending-end system.

$$\begin{cases} F_1 = F_{DC} - F_P \\ F_{DC} = \sum\limits_{i=1}^{N_G} P_G^i - \sum\limits_{j=1}^{N_{load}} P_{load}^j - \sum\limits_{k=1}^{N_{loss}} P_{loss}^k \\ F_P = \alpha N_{heavy} \end{cases} \tag{2}$$

where P_G^i, P_{load}^j and P_{loss}^k represent generator active power output, load level, and line active power loss, respectively. The introduction of the heavy-load severity F_P is to ensure stable operation of the sending-end system and maximize the uniform distribution of power flow. F_P is composed of the line heavy-load penalty coefficient α and the number of heavy-load lines N_{heavy}, which implies that the more transmission lines are heavily loaded, the more severe the penalty imposed, thereby forcing a more reasonable power flow distribution.

2.1.2. Renewable Energy Accommodation Capability of the Sending-End System F_2

As shown in Equation (3), F_2 is expressed as the sum of the current outputs of all wind and photovoltaic units in the sending-end system.

$$F_2 = \sum_{i=1}^{N_F} P_F^i + \sum_{j=1}^{N_G} P_G^j \tag{3}$$

where P_F^i and P_G^j represent the current active power output of wind farm i and photovoltaic station j, respectively.

2.1.3. Voltage Support Imbalance Degree (*VSID*) of the Sending-End System

Generally, as the output of renewable energy units increases, the MRSCR at their connection points will gradually decrease, bringing potential risks of voltage instability. Therefore, a reasonable regulation strategy is to increase the output of renewable energy units in regions with strong support capability to improve their accommodation level, while properly arranging wind and solar curtailment measures in regions with weak support capability, aiming to maintain the overall voltage support capability of the sending-end system in a balanced state. Accordingly, *VSID* of the sending-end system is given by Equation (4).

$$VSID = \sum_{i \in G_E} W_i (M_i - \overline{M})^2 \tag{4}$$

where G_E denotes all wind farms and photovoltaic stations; M_i and $\overline{M}$, respectively, represent the MRSCR of the point of interconnection (POI) of renewable energy stations i and the system average MRSCR; W_i is the curtailed wind or solar capacity of renewable energy stations i, which can eliminate the influence on the objective function caused by the hard constraints of units that have reached their rated output.

2.2. Constraints

During the optimization of external transmission power for DC sending-end systems, it is necessary to consider not only the fundamental constraints of system operation but also to ensure the support capabilities of the sending-end system.

2.2.1. Node Voltage Constraints

$$V_{i\min} \le V_i \le V_{i\max} \tag{5}$$

where $V_{i\min}$ and $V_{i\max}$ represent the lower and upper voltage limits at node i, respectively.

2.2.2. Voltage Support Capability Constraints at POI of Renewable Energy Stations

$$MRSCR_{\min} \le MRSCR_i \tag{6}$$

where $MRSCR_{\min}$ represents the minimum short-circuit ratio of the renewable energy station to prevent transient overvoltage from exceeding limits when a fault occurs in the vicinity of POI.

2.2.3. Frequency Support Capability Constraint of the Sending-End System

When large-scale DC blocking faults occur, the frequency fluctuations of the sending-end system must be constrained within permissible limits to prevent renewable energy sources from dragging the grid and triggering cascading failures [22]. This constraint is expressed as Equation (7).

$$f_N - f_{\min} \le \Delta f_{nadir} \le f_{\max} - f_N \tag{7}$$

where Δf_{nadir} represents the maximum transient frequency deviation after DC lockout, $f_{\min}$ denotes the minimum frequency constraint, and $f_{\max}$ denotes the maximum frequency constraint of the system.

2.2.4. Unit Output Constraints

$$P^i_{G\min} \le P^i_G \le P^i_{G\max} \tag{8}$$

where $P^i_{G\min}$ and $P^i_{G\max}$ represent the lower and upper limits of generator output, respectively. For renewable units, the lower limit is 0. To ensure sufficient synchronous frequency regulation capacity, the lower output limits for synchronous units participating in frequency regulation are set based on the maximum active power deficit during DC blocking fault.

$$\Delta P_{\max} \le \sum_{i=1}^{N_S} P^i_{S\min} + \sum_{j=1}^{N_H} P^j_{H\min} + \Delta P_{load} \tag{9}$$

where $P^i_{S\min}$ and $P^j_{H\min}$ represent the minimum outputs of hydro and thermal units participating in frequency regulation, respectively; ΔP_{load} denotes the active power surplus filled by load participation in frequency regulation after the fault occurs.

3. A Fast Optimization Framework for Unit Operation Mode of Asynchronous Interconnected Sending-End Power Systems Based on STGCN

The aforementioned UOMO model focuses on the operating state of the sending-end system at a specific moment. By adjusting the unit operation mode, it maximizes the transmission level of clean power while ensuring that the system voltage and frequency support capabilities satisfy the security constraints. In the daily operation scheduling of

the power grid, frequent disturbances such as load variations and output fluctuations of renewable energy units often occur. Therefore, an efficient solution method is urgently needed to meet the demand for operators to continuously and rapidly adjust the unit operation mode according to the time-series operating states of the sending-end system.

Accordingly, this section presents the optimization framework for the fast solution of the UOMO model, as illustrated in Figure 1. Centered on the data-driven deep learning prediction model STGCN, this framework learns from the time-series historical data of unit operation mode optimization in the sending-end system and fits the mapping relationship between the initial sectional state and the optimal target operation state of the system. Finally, based on the variation in the sending-end system operating state, the constructed STGCN model is adopted to achieve fast prediction of the unit operation mode.

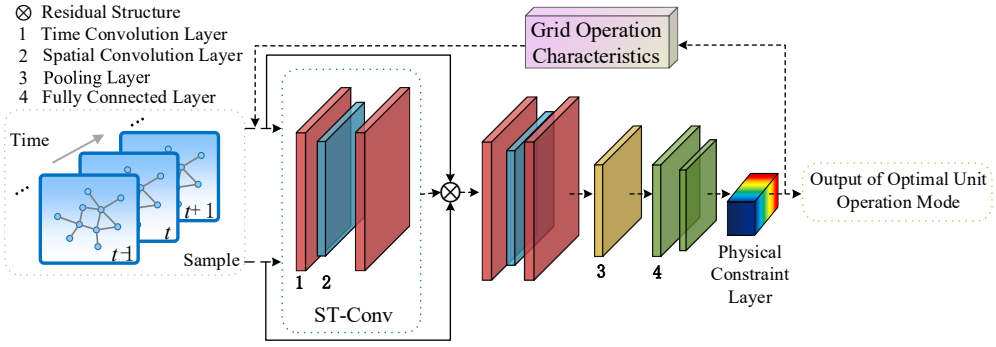


Figure 1. STGCN-based fast optimization framework for unit operation modes.

As shown in Figure 1, the optimization framework consists of two spatio-temporal graph convolutional blocks (ST-Conv) connected by residual structures, one pooling layer, five fully connected layers, one physical constraint layer, and a feedback mechanism incorporating the operation characteristics of the power grid. The main components of the framework are described in detail below.

3.1. The Construction of Spatio-Temporal Graph Convolutional Network

3.1.1. Spatial Graph Convolution Layer

Graph convolutional network (GCN) excels at aggregating information from neighbor nodes via the adjacency matrix and node feature matrix, which makes it highly suitable for processing graph-structured data in power grids.

The graph structure of a power grid can be defined as $G = (V, E, A)$, where V represents the set of nodes such as power plants and load nodes; E denotes the set of edges such as transmission lines; and A is the adjacency matrix, representing the connection relationships between nodes in the grid.

In the ST-Conv module shown in Figure 1, the input of the spatial graph convolutional layer is the node feature matrix output by the temporal convolutional layer. It is used to model the spatial correlation between nodes under a fixed power grid topology. The layer-wise propagation rule of GCN can be defined as:

$$\mathbf{H}^{(l+1)} = \sigma(\mathbf{D}^{-1/2}(\mathbf{A}+\mathbf{I})\mathbf{D}^{-1/2}\mathbf{H}^{(l)}\mathbf{W}^{(l)}) \tag{10}$$

where $\sigma(\cdot)$ is the activation function (e.g., ReLU); $\mathbf{H}^{(l)}$ denotes the input to layer l of graph convolution, namely the node feature matrix of layer l; $\mathbf{A}$ denotes the adjacency matrix of the power grid graph structure; $\mathbf{D}$ denotes the degree matrix of the power grid graph structure; $\mathbf{I}$ denotes the identity matrix; and $\mathbf{W}^{(l)}$ denotes the weight parameter matrix of layer l. The spatial graph convolution operation as shown in Equation (10) is used to perform spatial aggregation on node features at each time step and, together with the

preceding and subsequent temporal convolution layers, forms the ST-Conv module to realize the joint extraction of spatial–temporal features of power grid operating states.

3.1.2. Time Convolution Layer

To alleviate the impact of gradient descent and improve training efficiency, this paper employs a Gated Convolutional Neural Network (Gated CNN) with a Gated Linear Unit (GLU) to capture dynamic features of time series exhibited by units and loads during power system operation. In addition, residual connections are used to mitigate overfitting.

The temporal convolutional layer is designed as a one-dimensional causal convolution followed by a gated linear unit serving as the nonlinear layer. This architecture enables feature extraction from time series data of varying lengths. The incorporation of the gated linear unit effectively integrates linear and nonlinear transformations. The input to the temporal convolutional layer for each node comprises active power output and load data such as $\mathbf{X} \in \mathbf{R}^{M \times C_i}$, where M represents the length of the input time series and C_i denotes the number of selected electrical features. The convolutional kernel is designed as $\mathbf{\Gamma} \in \mathbf{R}^{k \times C_i \times 2C_0}$, performing a one-dimensional convolution operation on $\mathbf{X}$. The output can be defined as:

$$\mathbf{X}' = \mathbf{\Gamma} * \mathbf{X} = \mathbf{p} \otimes \sigma(\mathbf{q}) \in \mathbf{R}^{(M-k+1) \times C_0} \tag{11}$$

In Equation (11), $\mathbf{p}$ and $\mathbf{q}$ represent the inputs to each gate of the GLU, $\sigma(\cdot)$ denotes the activation function, C_0 indicates the number of output channels, and k specifies the size of the convolutional kernel.

3.1.3. Spatio-Temporal Graph Convolution Layer ST-Conv

To simultaneously extract complex dependencies across temporal and spatial dimensions in the unit operation optimization, the spatio-temporal graph convolutional layer (ST-Conv) is constructed by combining temporal gated convolutional layers and spatial graph convolutional layers. The architecture of ST-Conv is designed with a spatial layer sandwiched between two temporal layers, enabling rapid spatial state propagation between the two temporal convolutions. The ST-Conv structure is illustrated in Figure 2.

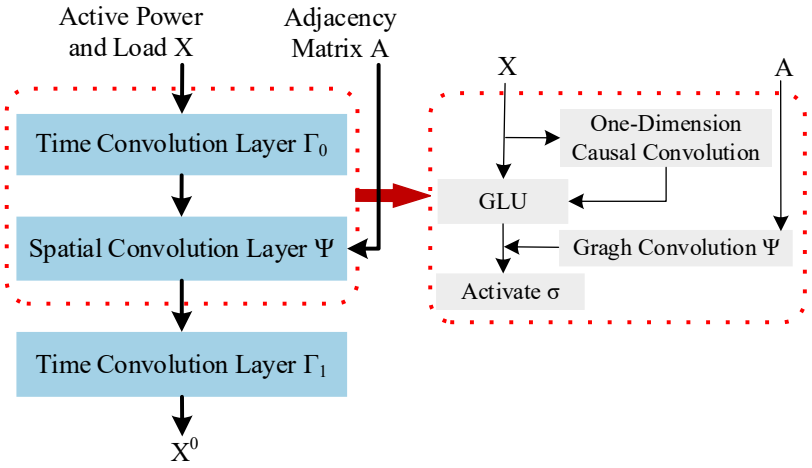


Figure 2. Spatio-temporal graph convolution layer.

The time convolution layer $\mathbf{\Gamma}_0$ in ST-Conv utilizes active power output and load data $\mathbf{X}$ as its inputs, employing the adjacency matrix of the power grid graph $\mathbf{A}$ as input for the spatial convolution layer $\mathbf{\Psi}$. First, the $\mathbf{X}$ is fed into the temporal convolutional layer $\mathbf{\Gamma}_0$, which employs one-dimensional causal convolution and GLU to capture temporal dependencies, performing convolution operations along the time dimension. Next, the obtained temporal features are combined with spatial features $\mathbf{A}$ obtained via $\mathbf{\Psi}$ through

an activation operation, implementing graph convolution in the spatial dimension. Subsequently, processing through the temporal convolution layer $\mathbf{\Gamma}_1$ further integrates temporal and spatial features, ultimately yielding the fused spatio-temporal features as shown in Equation (12):

$$\mathbf{X}^o = \mathbf{\Gamma}_1 * \sigma(\mathbf{\Psi} * (\mathbf{\Gamma}_0 * \mathbf{X}))) \tag{12}$$

ST-Conv not only extracts spatial features of the power grid but also integrates temporal characteristics during grid operation, providing robust support for comprehensive and reliable prediction of optimal unit operation modes.

3.2. Physical Constraint Layer and Feedback Mechanism Incorporating Operation Characteristics of Power Grid

To achieve fast prediction of the optimal unit operation mode using STGCN, it is necessary to efficiently and accurately learn the patterns of unit operation mode optimization. This requires further integrating the optimization objectives and partial operation constraints of UOMO model into the construction of STGCN, which is mainly implemented by the physical constraint layer and the feedback mechanism incorporating power grid operation characteristics in the optimization framework shown in Figure 1.

3.2.1. Physical Constraint Layer

The main physical constraints integrated into the optimization framework are: the power balance constraint shown as F_{DC} in Equation (2) at any time and the unit output constraints shown in Equations (8) and (9). In addition, since the proposed optimization framework requires continuous adjustment of the unit operation mode according to the time-series operating state of the sending-end system, it is also necessary to satisfy the ramp constraint of synchronous generators shown in Equation (13).

$$\begin{cases} -DR_i \leqslant P_{i,t} - P_{i,0} \leqslant UR_i, t = 1 \\ -DR_i \leqslant P_{i,t} - P_{t-1} \leqslant UR_i, t > 1 \end{cases}, \forall i \tag{13}$$

where UR_i and DR_i represent the operational ramping rate limits of the unit; $P_{i,t}$ and $P_{i,0}$ denote the output of the synchronous unit at time t and time 0, respectively.

Basic physical consistency constraints, including the power balance constraint and synchronous generator ramp-rate constraint mentioned above, are implemented by introducing a physical constraint layer into the STGCN architecture. This layer corrects the network prediction outputs via algebraic consistency modification so as to reduce the occurrence frequency of issues such as power imbalance or ramp-rate violations during the training process, thereby guiding the model to learn the mapping relationship that conforms to the operation mechanism of the power system.

For the unit output limit constraint, it is realized by applying constraint mapping to the predicted results of the fully connected layers at the output stage of the STGCN model, ensuring that the active power output of each unit always satisfies its limit requirements.

3.2.2. Feedback Mechanism Incorporating Operation Characteristics of Power Grid

For the overall objectives of the UOMO model, such as maximizing the DC transmission power and the output of renewable energy units as shown in Equations (2) and (3), the proposed optimization framework introduces corresponding penalty terms into STGCN loss function for soft constraint feedback guidance. By minimizing these loss terms, STGCN model is driven to improve its training speed while satisfying the aforementioned physical constraints and to generate unit operation mode prediction results that are more conducive to DC transmission and renewable energy accommodation.

The loss function $\mathcal{L}$ is modeled as Equation (14).

$$\mathcal{L} = \frac{1}{N}\sum_{i=1}^{N}|x_i - y_i| + \lambda_{DC}\mathcal{L}_{DC} + \lambda_{\text{res}}\mathcal{L}_{res} \tag{14}$$

where x_i and y_i represent the i-th actual value and predicted value, namely the mean of the unit output results generated by the model, respectively; λ_{DC} and λ_{res} are hyperparameters that balance the importance of the DC transmission loss and renewable energy accommodation loss terms, respectively, which should be properly adjusted according to the training performance. The DC transmission losses and renewable energy curtailment losses are defined as follows.

$$\mathcal{L}_{DC} = C_{DC} - \left(\sum_{i=1}^{N_G} P_G^i - \sum_{j=1}^{N_{load}} P_{load}^j\right) \tag{15}$$

$$\mathcal{L}_{res} = C_{\text{res}} - \left(\sum_{i=1}^{N_w} P_w^i + \sum_{j=1}^{N_{pv}} P_{pv}^j\right) \tag{16}$$

where C_{DC} and C_{res} are constants ensuring non-negativity of the loss function calculation; P_G^i is the active power output of the i-th unit; P_{load}^j is the magnitude of the j-th active load; and P_w^i and P_{pv}^j are the active power outputs of the i-th wind power unit and the j-th photovoltaic unit, respectively.

4. STGCN- and IMOPSO-PSD-Based Optimization Process for Unit Operation Mode of Asynchronous Interconnected Sending-End Power Systems

Using the optimization framework shown in Figure 1 to continuously adjust the unit operation mode according to the time-series operating state of the sending-end system requires completing the training of the STGCN model. First, a dataset available for the STGCN model needs to be constructed, which should contain the patterns or rules of optimal adjustment for the unit operation mode in the sending-end power system. Second, it can be observed that, due to the inherent characteristics of STGCN, its modeling does not incorporate the complete UOMO model. Thus, to ensure reasonable and effective results, the unit operation mode predicted by STGCN model requires further refining and verification.

In summary, the training process of STGCN model includes the main steps shown in Figure 3, namely, (1) construction of sequential sample sets based on IMOPSO-PSD; (2) training of the optimal unit operation mode prediction model based on STGCN; and (3) refining and validation of the prediction results based on the simplified IMOPSO-PSD.

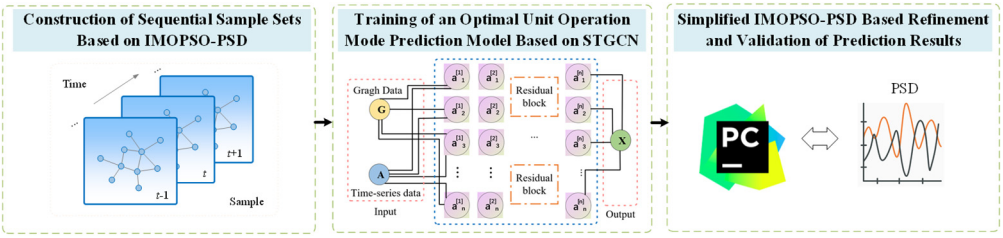


Figure 3. Optimization process for unit operation mode based on STGCN.

Next, the solution process of the UOMO model using IMOPSO-PSD serving as the foundation for steps (1) and (3) is introduced first. Subsequently, the key steps illustrated in Figure 3 are explained.

4.1. Solution of UOMO Model Based on IMOPSO-PSD and Its Simplified Process

UOMO model constructed in Section 2 is a nonlinear, multi-objective optimization problem. This paper proposes a solution method for UOMO model based on IMOPSO-PSD. The main optimization process is modeled using IMOPSO, which serves as the main optimization problem. The calculation of constraints such as the voltage support capability at POI of renewable energy stations involved in the model is solved using PSD software (Version 2.0.1.8) widely adopted by the dispatch departments of power companies, forming the optimization sub-problem. Upon completion of the main optimization process, the Pareto optimal solution set for unit operation modes is obtained, and the coefficient of variation method is further employed to determine the optimal unit operation mode. The complete solution process of UOMO model based on IMOPSO-PSD is illustrated in Figure 4.

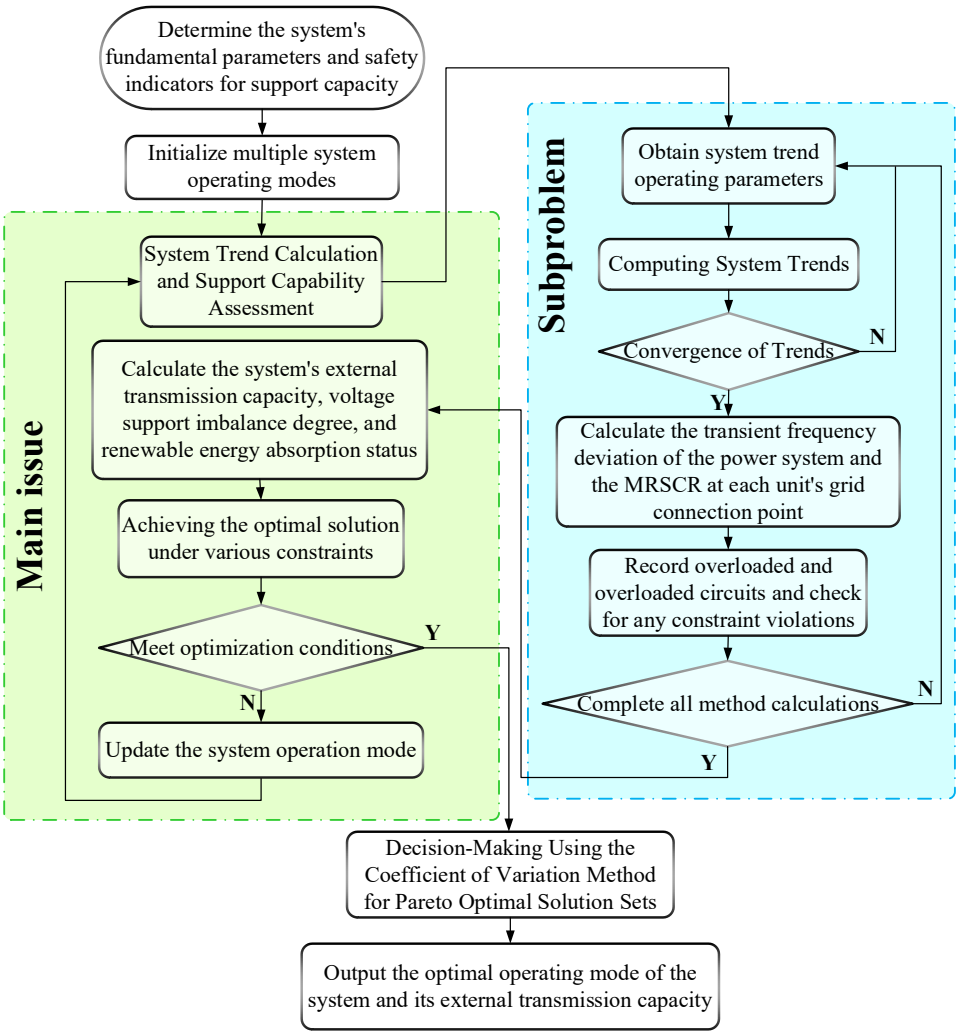


Figure 4. Solution process of UOMO model based on IMOPSO-PSD.

PSO algorithm features simple coding and strong adaptability to problems. IMOPSO algorithm adopted in this paper uses the same particle update mechanism as the standard PSO algorithm, where the velocity and direction of particles are determined according to the information of individual particles and the particle swarm in the solution space. The main improvements lie in suppressing the defect that the algorithm is prone to fall into local optima by introducing inertia weight, optimizing the selection of individual optimal values [23], and adopting crossover and mutation [24]. Meanwhile, infeasible solutions during initialization and optimization are avoided through timely constraint checking.

PSD software is a collection of power system analysis packages widely used in the dispatch departments of China's power grid companies. It includes many core programs such as the power flow calculation program PSD-PF, short-circuit current program PSD-SCCP, and transient stability program PSD-ST, with the advantages of large calculation scale and good numerical stability. Within the main problem-solving framework based on IMOPSO algorithm, PSD is used to calculate and verify sub-problems such as power flow calculation, MRSCR and transient frequency deviation, as shown in Figure 4.

The solution efficiency of UOMO model based on IMOPSO-PSD is significantly affected by the selection of initial solutions, and the solving process is time-consuming without prior heuristic information. However, when the initial solutions are relatively close to the target solutions, the necessary simplified procedure for IMOPSO-PSD is recommended to improve the solving efficiency. The simplified treatment includes reducing the size of the initial particle swarm, decreasing the number of iterations, and weakening mutation operations in the main optimization problem.

4.2. Construction of Labeled Sequential Sample Set Based on IMOPSO-PSD

A sequential sample set is a dataset of system operating states formed at a certain time resolution corresponding to a power grid topology represented by $G = (V, E, A)$, and its structure is a 4-dimensional matrix of size such as (NS, NN, NT, 2). Here, NS denotes the number of samples; NN denotes the number of nodes, which is equal to the total number of nodes in the node set V; NT denotes the length of the time-series data; and the number of node features is 2, representing the active power output and the node load at each node.

The sequential sample set consists of a relatively small number of typical scenarios and a large number of non-typical scenarios. The typical scenarios include representative operating states of the sending-end system in terms of the output levels of synchronous generating units, renewable energy units, load levels, and the corresponding outward transmission power levels. In addition, the typical scenarios also cover differentiated operating conditions such as fluctuations in renewable energy output. The non-typical scenarios refer to operating conditions that are close to the operating states of various typical scenarios, with the Euclidean distance as the quantitative criterion.

To enable STGCN model to learn the patterns or rules underlying the optimal adjustment of unit operation modes in the sending-end system contained in the sample set, it is necessary to optimize the unit operation modes for each time-series sample one by one to complete the labeling process. The labeling of a small number of typical scenarios is implemented through the solution flow of UOMO model based on IMOPSO-PSD. However, the labeling of a large number of non-typical scenarios is performed using a simplified IMOPSO-PSD flow. The reasons are as follows: during the labeling of typical scenarios, after multiple rounds of crossover and mutation operations of IMOPSO, a considerable number of suboptimal solutions are obtained along with the optimal solution for unit operation modes. Some of these suboptimal solutions may implicitly contain the optimal adjustment patterns for non-typical scenarios. Therefore, combined with quantitative judgment based on Euclidean distance, a certain number of suboptimal solutions can be selected to form an initial solution set together with non-typical scenarios, and the simplified IMOPSO-PSD can be used to quickly complete the labeling of non-typical scenarios.

4.3. Prediction Result Refinement and Verification Based on Simplified IMOPSO-PSD

Since STGCN model does not reflect the security constraints in UOMO model such as Equations (6) and (7), the predicted unit operation mode optimization results need to be refined and verified to ensure the accuracy and reliability.

To improve the efficiency of refinement and verification, some suboptimal solutions with prediction errors within a certain range from the STGCN prediction results are used as the initial solution set for the simplified IMOPSO-PSD procedure. The number and range of the solution set can be determined according to the prediction accuracy and reliability of STGCN model so that the optimal solution for unit operation mode optimization can be obtained rapidly.

5. Case Study

To demonstrate the effectiveness of the method proposed, IEEE 39-bus system, as shown in Figure 5, is modified to simulate a sending-end system with high penetration of renewable energy generators, which is interconnected with other regions via DC transmission lines.

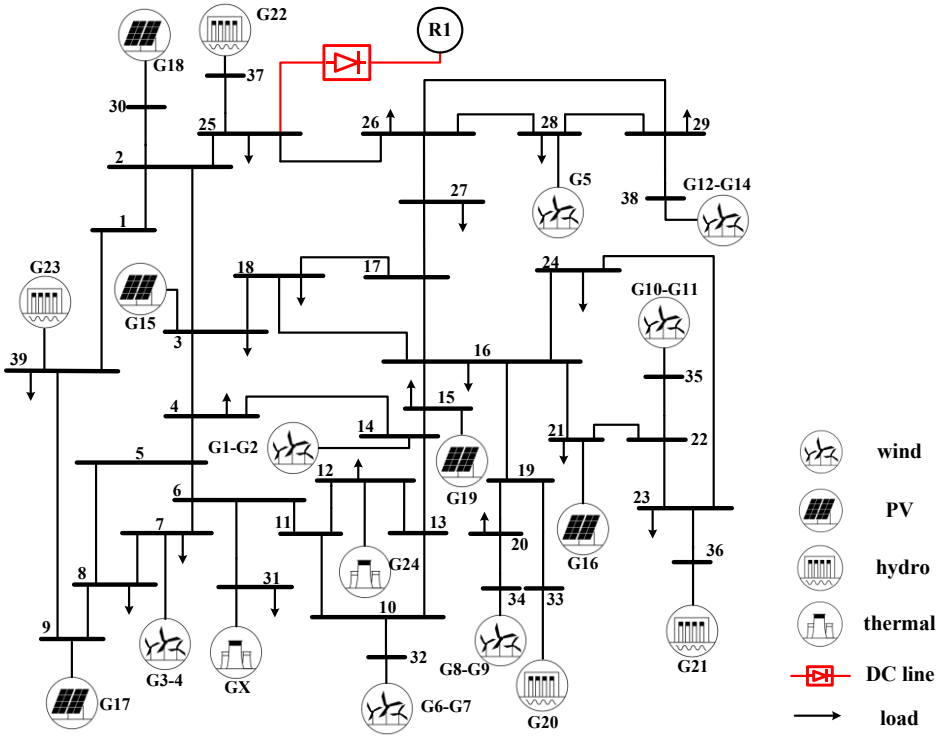


Figure 5. Modified IEEE 39-bus system diagram.

In the diagram, G1–G14 are wind turbines, G15–G19 are photovoltaic (PV) units, G20–G23 are hydroelectric units, and G24 and GX are thermal power units. GX serves as the balancing unit. The system is connected to an equivalent external system R1 through a single DC transmission line. To ensure the stability of the receiving-end system and maintain a sufficient load deficit, R1 is equivalent to an infinite bus system, and a large load is configured to simulate the power demand of a load center.

The total AC load inside the sending-end system is 3120.1 MW. The total installed capacity of renewable energy units is 3303 MW, and the total installed capacity of synchronous units is 3303 MW. The base capacity is 100 MVA, and the heavy-duty line flow limit is set to 90% of its rated value.

5.1. Sequential Sample Set

The objective of the unit operation mode optimization using the method proposed in this paper is to maximize the DC transmission level of clean green power while ensuring the voltage and frequency support capability of the sending-end system. Therefore, when constructing the sequential sample set, summer scenarios with relatively high output of

wind power, PV power and adequate hydropower are deliberately selected so as to avoid load shedding caused by insufficient wind and photovoltaic power generation during peak load periods.

Figure 6 shows the output of wind and PV units and the total load in the time-series sample set used for simulation in this paper. The sample adopts 15 consecutive days of operation data in the first half of June from a power grid, with a time resolution of 5 min and a total of 4320 samples. The training set and test set are divided at a ratio of 3:1. All samples have undergone the labeling process described in Section 4.2 to meet the requirements of subsequent STGCN model training and testing.

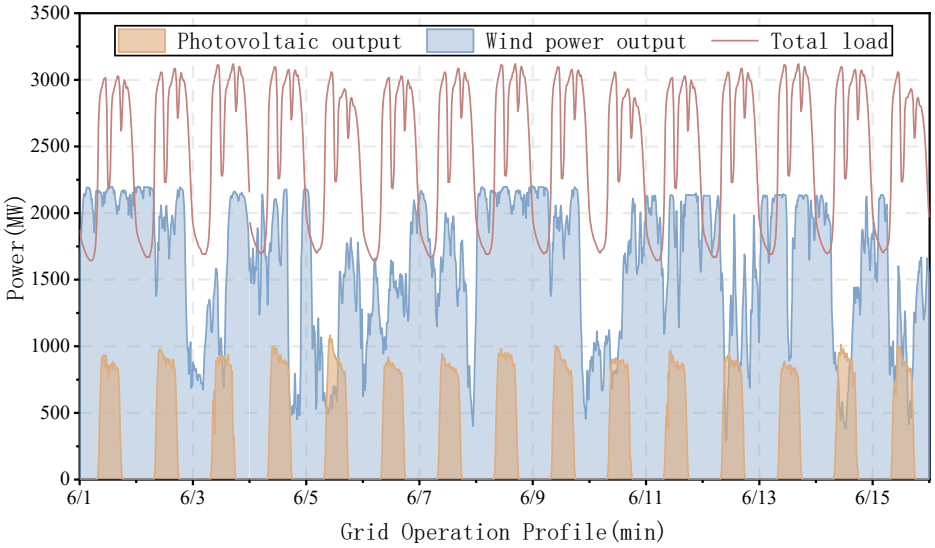


Figure 6. Sequential data used for case study.

5.2. Optimal Unit Operation Mode Prediction Based on STGCN Model

Based on PaddlePaddle, an open-source industrial-grade deep learning platform, STGCN model with the structure shown in Figure 1 has been built on the Python 3.7 platform. The experimental environment consists of an AMD Renoir (Ryzen 4000 APU) 4800H CPU @ 2.90 GHz, 16 GB of RAM, and an NVIDIA GeForce GTX 2060 GPU. The time stride is set to 12, the learning rate to 1×10^{-3}, and the number of features to 2.

Using the well-trained STGCN model, the prediction results of DC external transmission capacity and renewable energy accommodation capability are obtained by feeding the test dataset, as illustrated in Figure 7. The data marked with "Actual" represent the results obtained by solving DCEPTO model using IMOPSO-PSD or its simplified procedure, i.e., the label values of the input samples.

On the whole, the STGCN prediction model can effectively respond to the fluctuations in renewable energy generation. The prediction error of the optimal solution for unit operation modes is generally no more than 10%, and most errors are maintained within 5%. However, there still exist certain discrepancies between the model prediction results and the actual values during a few periods with large fluctuations in renewable energy. In addition, the prediction of DC external transmission capability at some moments is relatively conservative, indicating that room still exists for further improvement.

To further analyze the prediction performance of STGCN model, output prediction results of Unit 11 (wind power) and Unit 18 (photovoltaic), which exhibit relatively severe power fluctuations, are shown in Figure 8.

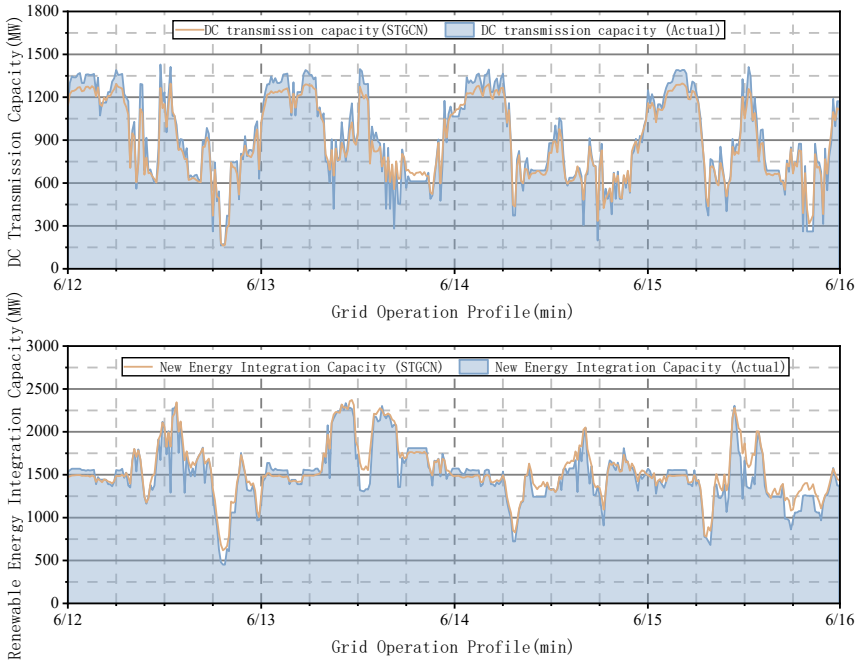


Figure 7. Prediction results of STGCN model.

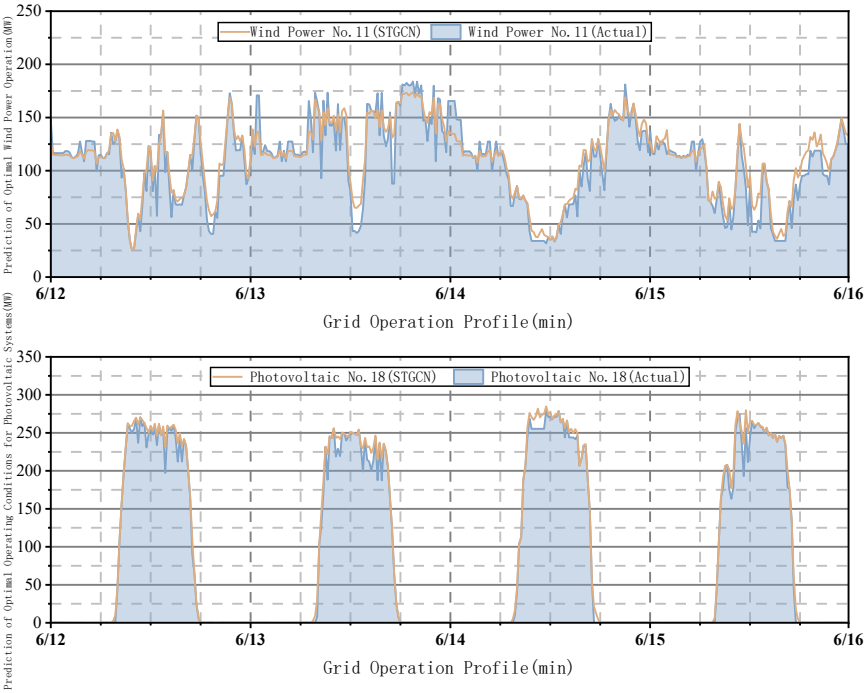


Figure 8. Output prediction of wind and photovoltaic units.

It can be observed that STGCN model can track the fluctuation trend of renewable energy units' output and ensure a certain prediction accuracy. Compared with PV units with relatively stable output, STGCN model has relatively large errors at individual moments when predicting the optimal outputs of wind power units with strong output fluctuations. If these results are directly adopted to adjust and control the unit operation, there exist potential risks such as insufficient voltage support capability and line flow violations.

5.3. Refinement of Prediction Results Based on Simplified IMOPSO-PSD

For the above optimization results with a few larger prediction errors, further refinement is required using the simplified IMOPSO-PSD procedure. Through comparative

simulation experiments, the main simplification measures adopted for the IMOPSO-PSD procedure include: reducing the initial particle population size by 40%, retaining only 10% of the original iterations, and removing inertia weight and crossover-mutation operations.

Based on the analysis of the prediction results from STGCN model, the prediction error range for samples to be refined is set to ±10%. That is, samples with prediction errors within ±10% are selected as the initial solutions for the simplified IMOPSO-PSD and further refined. The final optimization results are shown in Figure 9.

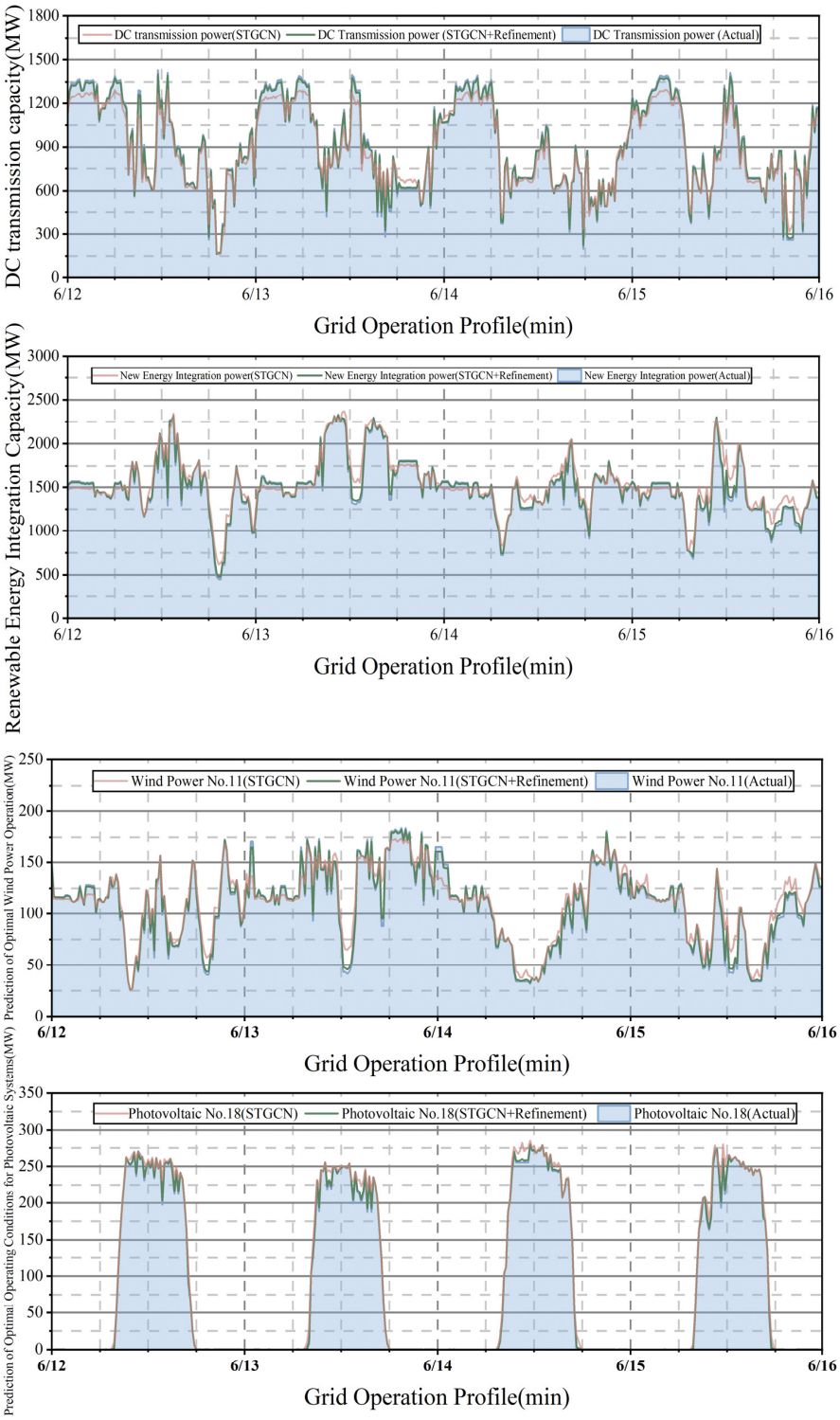


Figure 9. Refining performance of STGCN prediction results.

As shown in Figure 9, after further refinement, the prediction accuracy is significantly improved compared with the direct output of STGCN model. The optimized results are basically consistent with the actual values, except for a few peaks where the error is less than 5%. From the optimization results of individual units, even for Wind Turbine Unit 11 with relatively large output fluctuations, the maximum error between the refined output and the actual value is no more than 3%.

Furthermore, the reliability of refined prediction results is verified by comparing the MRSCR values at Wind Turbine Unit 14, where the voltage support capability is the weakest, as shown in Figure 10.

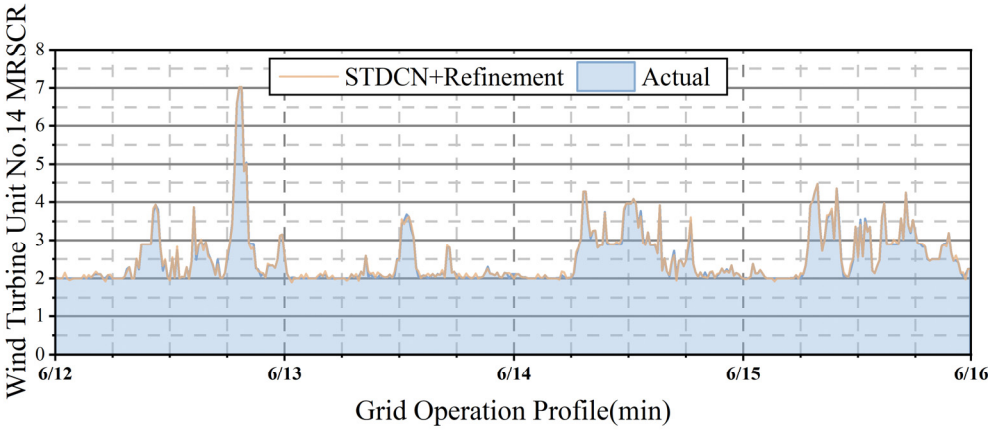


Figure 10. Comparison of MRSCR for Wind Turbine Unit No. 14.

As shown by the comparison between the refined predicted and actual MRSCR values, the proposed method can effectively regulate unit output. Even at the weakest voltage support location, the MRSCR remains above 2 for most periods and above 1.92 at its minimum, which guarantees the required voltage support for renewable energy units in the sending-end system.

5.4. Robustness Analysis of Proposed Method

Further, the robustness of the proposed method is analyzed by comparing the error statistical indicators between the direct prediction results of the STGCN model and the further refined results on the test dataset.

The test set contains a total of 1152 samples, including both typical and non-typical scenarios, which can reflect representative and differentiated system operating states. To avoid incomparable errors caused by differences in unit capacity, the absolute percentage error is adopted as the unified error evaluation index in this paper.

For the active power output of unit i under the k-th operating scenario, let its labeled value be $P_{i,k}^{act}$ and the result directly predicted by the STGCN model or further refined be $P_{i,k}^{opt}$. Then the relative error is defined as:

$$\varepsilon_{i,k} = \left| \frac{P_{i,k}^{opt} - P_{i,k}^{act}}{P_{i,k}^{act}} \times 100\% \right| \tag{17}$$

For the test dataset, the direct prediction results of STGCN model yield a mean relative error of 8.62%, a median of 3.92%, a variance of 167.66, and a standard deviation of 12.97. It can be observed from unit outputs of samples that STGCN model produces relatively large prediction errors for scenarios with severe output fluctuations of renewable energy units. The large variance and standard deviation of the relative errors indicate that the robustness of the model needs to be improved.

Furthermore, after refining the prediction results of STGCN model using the simplified IMOPSO-PSD procedure, the mean relative error is 1.44%, the median is 0.65%, the variance is 4.66, and the standard deviation is 2.16. It can be seen that both the accuracy and stability of the final solution are significantly improved, which ensures the reliability for practical applications.

6. Conclusions

Based on the operational characteristics and dispatching requirements of asynchronous networking sending-end power systems with high-penetration renewable energy, this paper proposes a fast optimization method for unit operation modes based on STGCN and IMOPSO-PSD. It completes the construction of a multi-objective optimization model, the design of an STGCN framework integrated with physical constraints, and the realization of the full-process optimization, with the effectiveness of the method verified through case analysis on the modified IEEE 39-bus system. The main conclusions are as follows:

(1) The constructed UOMO model balances multiple objectives, including DC power transmission, renewable energy accommodation and voltage support balance, incorporates voltage and frequency support capabilities, as well as unit operation security constraints, and accurately meets the collaborative optimization requirements of "security-accommodation-transmission" for asynchronous networking sending-end systems, thus providing a scientific model foundation for the optimization of unit operation modes.

(2) The STGCN framework integrated with a physical constraint layer and a feedback mechanism for objective loss of UOMO can effectively extract the spatial dependence of grid node topology and the temporal dependence features of generation load. Its prediction results can well track the fluctuation trend of renewable energy output. The mean error of the predicted optimal solution for unit operation mode is within 10%, which can provide high-quality initial solutions for subsequent refinement. This significantly alleviates the initial-value sensitivity issue of traditional intelligent optimization methods and greatly improves optimization efficiency.

(3) The refining strategy for STGCN prediction results based on the simplified IMOPSO-PSD procedure is effective. Compared with the prediction results of STGCN model, it significantly reduces the prediction deviation under scenarios with severe fluctuations in renewable energy output. The accuracy and stability of the solutions are both remarkably improved, ensuring reliability in practical applications.

In summary, the proposed method not only leverages the fast spatio-temporal feature extraction and prediction capability of STGCN but also ensures the physical rationality of the optimization results by using the accurate constraint checking ability of IMOPSO-PSD. This can meet the needs of operators for continuous and rapid adjustment of unit operation modes and also provides a new solution for power system optimization problems.

Although the proposed method for optimizing unit operation modes of asynchronous interconnected sending-end power systems has achieved preliminary performance, its adaptive capability for engineering applications still needs to be further enhanced. Future improvements are discussed as follows:

(1) A comprehensive operation-mode sample set is essential to improve the prediction performance of STGCN model, which is inherent to deep-learning methods. On the one hand, representative operating scenarios with sufficient security margins and high clean-energy DC transmission levels should be collected, with particular attention to complex cases such as rapid fluctuations in renewable energy generation under extreme weather. On the other hand, the optimal and suboptimal operation modes predicted by STGCN can be fed back into the sample set as high-quality samples to serve as initial solutions and boost training efficiency.

(2) The proposed method is currently validated under a fixed grid topology, where only generation output is optimized without considering unit commitment. To achieve full and flexible regulation of system operation modes, the capability of STGCN in modeling variable grid topologies should be further explored, and security constraints related to unit start–stop should be incorporated into the model.

Finally, based on the above improvements, the engineering applicability of the model to large-scale practical power grids will be investigated.

Author Contributions: Conceptualization, D.Z. and Y.L.; methodology, D.Z. and Y.L.; validation, Y.L. and X.Z.; investigation, X.Z. and K.Y.; writing—original draft preparation, D.Z., Y.L., W.W. and K.X.; writing—review and editing, D.Z., Y.L. and K.Y.; project administration, D.Z. All authors have read and agreed to the published version of the manuscript.

Funding: This work receives funding from Science and Technology Project of China Southern Power Grid Co., Ltd. Project No. 050100KC24100021.

Data Availability Statement: The data used to support the findings of this study are included within the article.

Conflicts of Interest: Mr. Dan Zhang and Ms. Kaiyuan Yu are employed by China Southern Power Grid Yunnan Power Grid Co., Ltd. The remaining authors declare that they have no known competing financial or non-financial interests that could have influenced the work reported in this manuscript.

Nomenclature

STGCN	spatio-temporal graph convolutional network
IMOPSO-PSD	multi-objective particle swarm optimization–power system department software
UOMO	unit operation mode optimization
MRSCR	multiple renewable energy stations short circuit ratio
VSID	voltage support imbalance degree

References

1. Zhou, B.R.; Rao, H.; Wu, W.; Wang, T.; Hong, C.; Huang, D.Q.; Yao, W.F.; Su, X.R.; Mao, T. Principle and Application of Asynchronous Operation of China Southern Power Grid. *IEEE J. Emerg. Sel. Top. Power Electron.* **2018**, *3*, 1032–1040. [CrossRef]
2. Rao, H.; Wu, W.; Mao, T.; Zhou, B.R.; Hong, C.; Liu, Y.J.; Wu, X.S. Frequency Control at the Power Sending Side for HVDC Asynchronous Interconnections Between Yunnan Power Grid and the Rest of CSG. *CSEE J. Power Energy Syst.* **2021**, *1*, 105–113. [CrossRef]
3. Xu, X.; Zhang, K.; Bian, J.; Li, J.; Chen, H. Operation Optimization of Multi-Energy Complementary Systems Considering Output Characteristics of Large-Scale Multi-Regional Clean Energy Bases at the Sending End. In Proceedings of the 2025 International Conference on Applied Electrical Engineering and Technology (AEET), Taiyuan, China, 29–31 August 2025; pp. 391–395. [CrossRef]
4. Li, J.; Song, X.; Zhang, Y.; Gao, F. Operation optimization of active distribution network considering maximum consumption of distributed generation. In Proceedings of the 2019 IEEE 8th International Conference on Advanced Power System Automation and Protection (APAP), Xi'an, China, 21–24 October 2019; pp. 1053–1057. [CrossRef]
5. Yang, D.; Li, Q.; Yao, Z.; Li, J.; Zhao, Y.; Yang, Y. Multi-Objective Optimization of Improved Particle Swarm Optimization Considering Economic and Environmental Indexes of CCHP System. In Proceedings of the 2024 Second International Conference on Cyber-Energy Systems and Intelligent Energy (ICCSIE), Shenyang, China, 17–19 May 2024; pp. 1–5. [CrossRef]
6. Baimakhanov, O.; Saukhimov, A.; Ceylan, O. Whale Optimization Algorithm Based Optimal Operation of Power Distribution Systems. In Proceedings of the 2022 57th International Universities Power Engineering Conference (UPEC), Istanbul, Turkey, 30 August–2 September 2022; pp. 1–6. [CrossRef]
7. Abdalla, O.H.; Mohamed, A.A.; Abdo, M.H. Optimal Operation of a Microgrid with Osprey Optimization Algorithm. In Proceedings of the 2024 25th International Middle East Power System Conference (MEPCON), Cairo, Egypt, 17–19 December 2024; pp. 1–6. [CrossRef]
8. Porubay, O.; Siddikov, I. Algorithms for Optimization of Operation Modes of Electric Power Systems Under Conditions of Information Uncertainty. In Proceedings of the 2024 International Conference on Information Science and Communications Technologies (ICISCT), Seoul, Republic of Korea, 7–8 November 2024; pp. 320–325. [CrossRef]

9. Li, J.; Zhu, Y.; Ye, Z.; Hu, X.; Gong, X. Design and Application of Multi Objective Optimization Algorithm in Optimization of Distribution Network Operation Mode. In Proceedings of the 2025 International Conference on Advances in Electrical Engineering and Computer Applications (AEECA), Dalian, China, 22–24 August 2025; pp. 112–117. [CrossRef]
10. Zhao, L.; Yin, C.; Sheng, F.; Sun, Y.; Chen, P.; Dai, H. Operation Optimization for Power System with Multiple Reserve Resources Based on Deep Reinforcement Learning. In Proceedings of the 2025 International Conference on New Power System Technology (PowerCon), Hefei, China, 24–25 September 2025; pp. 1–5. [CrossRef]
11. Locher, L.; Stai, E.; Hug, G. A Safe Combined Reinforcement Learning and Model Predictive Control Scheme for Utility-Level Battery Control in Distribution Grids. *IEEE Trans. Smart Grid* **2026**, *17*, 144–160. [CrossRef]
12. Hu, Z.; Zhang, H. A Transparent Neural Network Solver for Optimal Power Flow Problem. *IEEE Trans. Power Syst.* **2026**, *41*, 54–69. [CrossRef]
13. Zhao, D.M.; Wu, J.Q.; Song, C.M.; Wang, Y.; Wan, J.B.; Chang, G.Y. Transient Frequency Stability Assessment Based on Improved Spatial-Temporal Graph Convolutional Network. *J. N. China Electr. Power Univ. (Nat. Sci. Ed.).* Available online: https://link.cnki.net/urlid/10.1999.TM.20250707.1624.004 (accessed on 10 February 2026).
14. Cheng, X.C.; Liu, J.X.; Kang, R.K. Ultra-Short-Term Wind Power Forecasting Based on Improved STGCN and N-BEATS. *Mod. Electron. Technol.* **2025**, *48*, 115–121. [CrossRef]
15. Li, L.G.; Sun, L.Q.; Dai, Y.S. A Method for Ultra-Short-Term Prediction of Photovoltaic Power Generation Based on Spatiotemporal Graph Convolutional Neural Networks. *Therm. Power Eng.* **2023**, *38*, 152–157+173. [CrossRef]
16. Zhai, H. Re-STGCN Based Short-Term Voltage Stability Assessment in Regional Power Systems. In Proceedings of the 2025 IEEE 8th International Electrical and Energy Conference (CIEEC), Changsha, China, 16–18 May 2025; pp. 1747–1752. [CrossRef]
17. Feng, K. A Frequency Stability Prediction Method Using Spatial Temporal Graph Convolutional Networks and Self-attention Mechanism. In Proceedings of the 2024 6th International Conference on Electrical Engineering and Control Technologies (CEECT), Shenzhen, China, 20–22 December 2024; pp. 109–113. [CrossRef]
18. Qin, K. Self-attention STGCN-based Interpretability Method for Frequency Stability Prediction. In Proceedings of the 2024 6th International Conference on Power and Energy Technology (ICPET), Beijing, China, 12–15 July 2024; pp. 462–467. [CrossRef]
19. Zhou, Z.; Li, H.; Zheng, J.; Xiang, X.; Yao, R.; Tan, H. Power System Frequency Response Prediction with Spatial-Temporal Graph Convolutional Networks. In Proceedings of the 2025 IEEE International Conference on Electrical Energy Conversion Systems and Control (IEECSC), Chongqing, China, 23–25 May 2025; pp. 453–459. [CrossRef]
20. Qin, J.T.; Yang, R.; Yu, N.P. Physics-Informed Graph Neural Networks for Collaborative Dynamic Reconfiguration and Voltage Regulation in Unbalanced Distribution Systems. *IEEE Trans. Ind. Appl.* **2025**, *61*, 2538–2548. [CrossRef]
21. Sun, H.D.; Xu, S.Y.; Xu, T.; Guo, Q.; He, J.; Zhao, B.; Yu, L.; Zhang, Y.; Li, W.; Zhou, Y.; et al. Definition and index of short-circuit ratio of new energy multi-field stations. *Chin. J. Electr. Eng.* **2021**, *41*, 497–506.
22. He, H.L.; Zhang, Y.T.; Sun, X.Q.; Guo, Q.; Sun, L.; Wang, Y.; Wang, M.; Huang, B. A method to evaluate the scale of new energy development and DC outgoing transmission in northwest power grid considering frequency safety constraints. *Chin. J. Electr. Eng.* **2021**, *41*, 4753–4762.
23. Tao, J.; Xu, W.; Li, Y.L.; Huo, Y.W.; Zhang, E.M. Optimal operation of integrated energy system combined cooling heating and power based on multi-objective algorithms. *Chin. J. Sci. Technol. Eng.* **2019**, *19*, 200–205.
24. Wu, X.G.; Liu, Z.Q.; Tian, L.T.; Ding, D.; Yang, S.L. Energy Storage Device Locating and Sizing for Distribution Network Based on Improved Multi-Objective Particle Swarm Optimizer. *Chin. J. Power Syst. Technol.* **2014**, *38*, 3405–3411. [CrossRef]

Disclaimer/Publisher's Note: The statements, opinions and data contained in all publications are solely those of the individual author(s) and contributor(s) and not of MDPI and/or the editor(s). MDPI and/or the editor(s) disclaim responsibility for any injury to people or property resulting from any ideas, methods, instructions or products referred to in the content.